Molecular Biology of the Cell
Vol. 20, 1728–1736, March 15, 2009

A Primary Role for Golgi Positioning in Directed Secretion, Cell Polarity, and Wound Healing

Smita Yadav, Sapna Puri, and Adam D. Linstedt

Department of Biological Sciences, Carnegie Mellon University, Pittsburgh, PA 15213

Submitted October 29, 2008; Revised December 19, 2008; Accepted January 13, 2009
Monitoring Editor: Jennifer Lippincott-Schwartz

Peri-centrosomal positioning of the mammalian Golgi apparatus is known to involve microtubule-based motility, but its importance for cellular physiology is a major unanswered question. Here, we identify golgin-160 and GMAP210 as proteins required for centripetal motility of Golgi membranes. In the absence of either golgin, peri-centrosomal positioning of the Golgi apparatus was disrupted while the cytoskeleton remained intact. Although secretion persisted with normal kinetics, it was evenly distributed in response to wounding rather than directed to the wound edge. Strikingly, these cells also completely failed to polarize. Further, directionally persistent cell migration was inhibited such that wound closure was impaired. These findings not only reveal novel roles for golgin-160 and GMAP210 in conferring membrane motility but also indicate that Golgi positioning has an active role in directed secretion, cell polarity, and wound healing.

INTRODUCTION

Juxtanuclear positioning of the Golgi apparatus is a striking feature of the interphase mammalian cell. Golgi membranes are largely confined to a region surrounding the centrosome or microtubule-organizing center (MTOC) and the positioning of the MTOC and its aster of microtubules largely determines the positioning of the Golgi apparatus. In the absence of microtubules the Golgi ribbon is fragmented and reorganizes into numerous distributed "ministacks," which, nevertheless, remain competent for processing and secretion (Thyberg and Moskalewski, 1999). On microtubule reassembly, Golgi membranes appear to be captured by outgrowing microtubule plus ends and then translocate inward (Vaughan *et al.*, 2002). The minus-end–directed movement is mediated by the dynein and dynactin motor complex (Burkhardt *et al.*, 1997; Roghi and Allan, 1999; King and Schroer, 2000). Once positioned near microtubule minus ends the Golgi membranes undergo homotypic fusion and lateral linking to form the ribbon-like membrane network. The Golgi ribbon may also be anchored directly to microtubule minus ends and/or centrosomes, further contributing to its peri-centrosomal positioning (Infante *et al.*, 1999; Takahashi *et al.*, 1999).

Significantly, certain extracellular stimuli induce repositioning of both the Golgi apparatus and the MTOC yielding a striking alignment with respect to the stimulus (Kupfer *et al.*, 1982; Pu and Zhao, 2005). Migrating fibroblasts respond to wounding, or to a chemotactic gradient, or even to an electric field, such that the Golgi apparatus and the MTOC are repositioned to face the direction of migration, i.e., the cell's leading edge (Kupfer *et al.*, 1982). Natural killer cells form an immunological synapse with target cells in which they release lytic factors that kill the target cell. During this process Golgi membranes and the MTOC are repositioned to face the area of cell–cell contact (Kupfer *et al.*, 1983). Axon formation in hippocampal cells occurs opposite the plane of cell division and at a site faced by the Golgi apparatus and the MTOC (de Anda *et al.*, 2005).

The rapid and synchronized reorientation of the Golgi along with the MTOC is thought to facilitate polarized secretion thereby providing membrane and secreted products directly to the most proximate plasma membrane such as the leading edge in migrating cells (Bergmann *et al.*, 1983), the immunological synapse in natural killer cells, and the developing axonal neurite in hippocampal neurons. However, a required role for Golgi peri-centrosomal positioning has not been demonstrated, and it is conceivable that factors such as the polarized cytoskeleton and vesicle fusion sites localized to the leading edge are sufficient to sustain the polarized state. What is known is that secretion is required (Bershadsky and Futerman, 1994; Prigozhina and Waterman-Storer, 2004) and that secretion becomes directed to the leading edge during the polarity response (Schmoranzer *et al.*, 2003). Microtubule depolymerization blocks focused secretion, polarity, and directed migration (Vasiliev *et al.*, 1970; Goldman, 1971; Rodionov *et al.*, 1993; Schmoranzer *et al.*, 2003), but, obviously, microtubule depolymerization causes the loss of both the cytoskeleton and Golgi positioning. It was also recently found that phosphorylation of the Golgi structural protein GRASP65 is required for MTOC and Golgi reorientation (Bisel *et al.*, 2008) and that GRASP65 is part of a complex controlling a kinase required for cell migration (Preisinger *et al.*, 2004). Although these observations suggest that Golgi remodeling and/or Golgi based signaling are required during the establishment of polarity they do not address the question of whether Golgi peri-centrosomal positioning, itself, is needed for directed secretion and polarity.

Therefore, to test the role of Golgi positioning we sought an experimental condition that specifically disrupts Golgi positioning without causing microtubule disassembly. Toward this end we depleted certain golgins, which are coiled-coil proteins associated with the cytoplasmic face of the

This article was published online ahead of print in *MBC in Press* (http://www.molbiolcell.org/cgi/doi/10.1091/mbc.E08–10–1077) on January 21, 2009.

Address correspondence to: Adam D. Linstedt (linstedt@andrew.cmu.edu).

Supplemental Material can be found at:
http://www.molbiolcell.org/content/suppl/2009/01/21/E08-10-1077.DC1

Golgi membrane, as some golgins may recruit or activate motors involved in Golgi positioning (Barr and Short, 2003). Indeed, knockdown of the golgin GMAP210 has been shown to disperse the Golgi (Rios *et al.*, 2004), and in an siRNA screen we identified GMAP210, as well as another golgin, golgin-160, as components whose knockdown significantly fragmented and dispersed the Golgi apparatus without disassembly of the microtubule or actin cytoskeletal systems. Secretion kinetics appeared normal. However, strong defects were observed in the direction of secretion in response to wounding and in cell polarization and cell migration demonstrating that Golgi positioning is critical in various aspects of cell polarity.

MATERIALS AND METHODS

Cell Culture, Transfection, and Materials

Reagents were from Sigma-Aldrich (St. Louis, MO) unless stated otherwise. HeLa cells were grown in minimal essential medium containing 10% fetal bovine serum, 100 IU/ml penicillin-G, and 100 μg/ml streptomycin at 37°C and 5% CO_2. All siRNA transfections were performed using Oligofectamine (Invitrogen, Carlsbad, CA) according to manufacturer's specifications. A nonspecific siRNA and an siRNA targeting p115 were used as negative and positive controls, respectively (Puthenveedu and Linstedt, 2004). The golgin-160 mRNA sequence targeted in most experiments was 5′-AAGGUGGAAGCCGGGCAUAAC-3′. Other targeted sequences yielding the same phenotype were 5′-AAGGCCTACGAGAACGCCGTG-3′ and 5′-AAGATCCCGGACTGCCCAGTT-3′. The siRNAs targeting GMAP210 were as published (Rios *et al.*, 2004). For gene replacement, cells were transfected with the replacement construct 72 h after siRNA transfection using Transfectol (GeneChoice, Frederick, MD). Silent mutations were introduced into the parent myc-tagged plasmid (Hicks and Machamer, 2002) to confer resistance to knockdown using the forward primer 5′-GGTCGAGGCCGGCCATAACCGCCGC-3′ according to the QuickChange protocol (Stratagene, La Jolla, CA). Antibodies used were anti-γ-tubulin (Sigma), anti-α-tubulin (Sigma), anti-acetylated-tubulin (Sigma), anti-golgin-160 (Hicks and Machamer, 2002), anti-GRASP65, and anti-GMAP210 (BD Biosciences, San Jose, CA). Rhodamine-phalloidin (Molecular Probes, Eugene, OR) was used for F-actin staining, and the nucleus was stained with Hoechst-33258 (Sigma).

Vesicular Stomatitis Virus Glycoprotein–Green Fluorescent Protein Transport Assay

HeLa cells stably expressing the temperature-sensitive mutant vesicular stomatitis virus glycoprotein (VSVG)–green fluorescent protein (GFP) under the control of a Tet promoter (Feinstein and Linstedt, 2008) were siRNA transfected, and after 48 h they were induced for 24 h using 0.5 μg/ml doxycycline. The cells were shifted to 40°C for 20 h to accumulate VSVG-GFP in the endoplasmic reticulum (ER), then shifted to 20°C for 2 h to allow transport to the *trans*-Golgi network (TGN), and finally shifted to 32°C for various times to allow surface transport. Staining was as previously described (Puthenveedu *et al.*, 2006). The ratio of surface-to-total fluorescence was used to calculate the extent of VSVG transport as described (Puthenveedu and Linstedt, 2004).

Wound-Healing Assays

Confluent cell monolayers, grown on 22 × 22-mm coverslips, were scraped using a 200-μl pipette tip to form a scratch wound (250-μm average width). Transfection with siRNA was carried out 48 h before wounding. Marker analysis and VSVG-GFP transport assays were carried out 6 h after wounding to ascertain polarity. To determine the extent of cell migration into the wound area the cells were fixed 17 h after wounding.

Microscopy and Image Analysis

Transmission electron microscopy was performed on cells fixed in 2.5% glutaraldehyde at room temperature for 30 min and then further processed using a permanganate contrast protocol (Puthenveedu *et al.*, 2006). Confocal images were acquired using an Axiovert 200 with a 100× Plan-Apo NA 1.4 oil objective (Zeiss, Thornwood, NY) attached to an UltraView spinning-disk confocal system (Perkin Elmer-Cetus, Shelton, CT). The number of fluorescent objects per cell was determined using a fixed threshold and the "Analyze Particle" plugin in ImageJ (http://rsbweb.nih.gov/ij). Fluorescence intensity of Golgi objects after BFA washout was determined using fixed threshold and background subtraction to exclude ER-localized fluorescence, images were acquired with an epifluorescence microscope with a 40× oil immersion lens (Linstedt *et al.*, 1997). The ImageJ "Measure" function yielded object area and average intensity, which were multiplied and the resulting product was summed for each cell. Secretion polarity was quantified using the ImageJ plug-in "Azimuthal Average" by dividing the best fitting circle around each cell into four quadrants and plotting the integrated fluorescence intensity over each degree radian. Golgi membrane motility was quantified for at least 20 Golgi objects per cell using the ImageJ plugin "MTrackJ" (http://www.imagescience.org/meijering/software/mtrackj/). Images were acquired at 90-s intervals during nocodazole washout. Displacement distance was the vector magnitude described by the final and initial coordinates of each object.

Statistical Analysis

For all statistical analysis, the data are obtained from experiments done in triplicate and Student's *t* tests were performed taking into account the two-tailed distribution and two-sample unequal variance of the pooled data.

RESULTS

An siRNA screen carried out in HeLa Cells stably expressing the Golgi enzyme galactosyl N-acetyl transferase-2 tagged with green fluorescent protein (GalNAcT2-GFP) identified golgin-160 and GMAP-210 as proteins whose knockdown

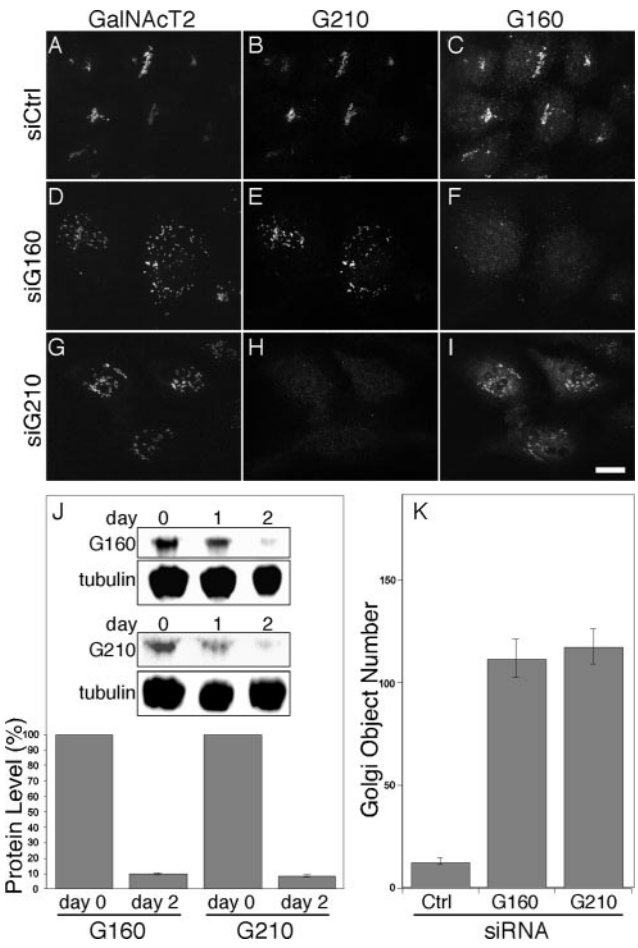

Figure 1. Depletion of golgin-160 and GMAP210 fragments the Golgi apparatus. (A–I) HeLa cells expressing GalNAc T2-GFP were treated with control siRNA (A–C), golgin-160 siRNA (D–F), or GMAP210 siRNA (G–I) and then costained with anti-golgin 160 and anti-GMAP210 antibodies. Bar, 10 μm. (J) Cell lysates prepared from cells 0, 1, or 2 d after transfections with golgin-160 or GMAP210 siRNAs analyzed by immunoblotting to assay golgin-160, GMAP210, and tubulin levels. The inset shows representative immunoblots, and the average extent of knockdown is plotted for multiple experiments (±SEM, n = 3). (K) The number of Golgi objects determined by automated fluorescent object counting was plotted for control, golgin-160, or GMAP210 knockdown cells. Values are averages (±SEM, n = 15).

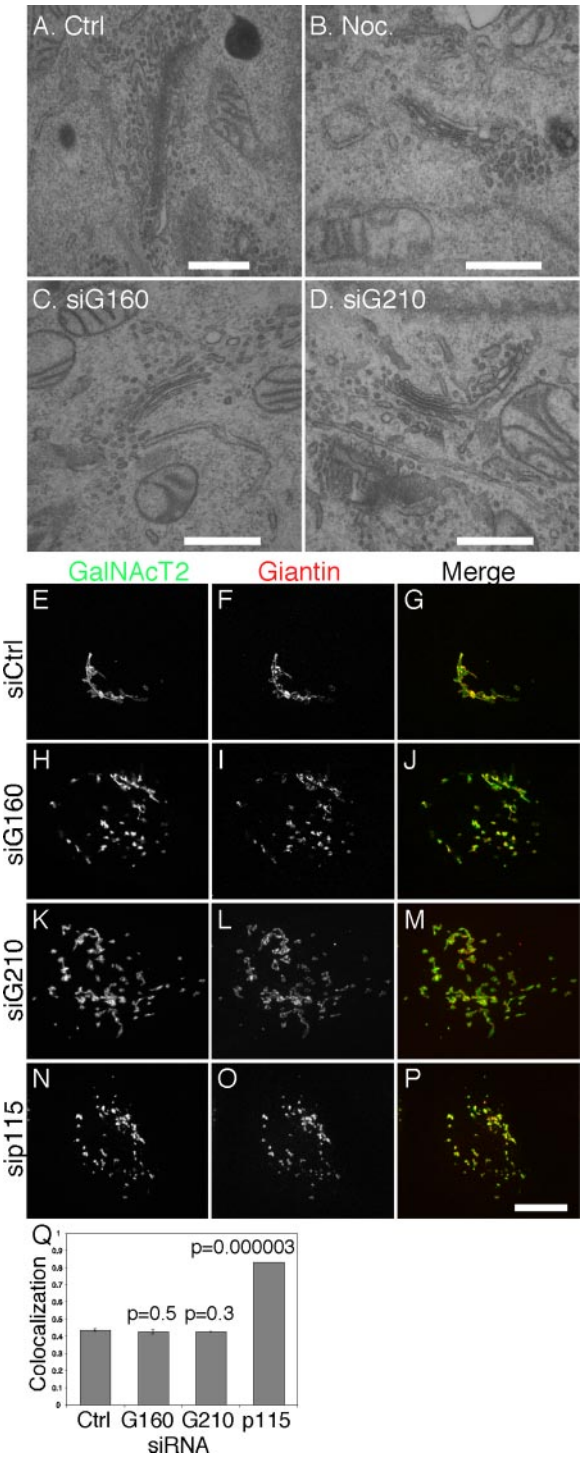

Figure 2. Depletion of golgin-160 or GMAP210 yields dispersed Golgi ministacks. (A–D) Cells treated with control siRNA (A), 0.5 μg/ml nocodazole for 3 h (B), golgin-160 siRNA (C), or GMAP210 siRNA (D) were analyzed by transmission electron microscopy. Bars, (A–D) 0.5, 0.1, 0.1, and 0.1 μm, respectively. (E–P) Control siRNA-treated cells (E–G) or cells depleted of golgin-160 (H–J), GMAP210 (K–M), or p115 (N–P) were stained and imaged to detect GalNAcT2-GFP and giantin. Merged images are also shown. Bar, 10 μm. (Q) Marker segregation was determined using the colocalization plugin of ImageJ, and the percentage of coincident pixels was compared. P values are indicated for comparison to the siRNA control sample and support persistent segregation after golgin, but not p115, knockdown.

led to scattering of Golgi-membranes. In the case of GMAP-210 this agreed with previous work (Rios *et al.*, 2004). Figure 1, A–I, compares the GalNAcT2-GFP pattern for cells transfected with control, golgin-160, and GMAP210 siRNAs and shows the staining level of each golgin. Despite the fragmented and distributed Golgi apparatus, the cells were viable and continued to divide. Dispersed Golgi membranes were evident in ~90 and 75% of golgin-160 and GMAP210 siRNA transfected cells, respectively, and only cells with significant staining loss exhibited the phenotype. Correlation of phenotype with knockdown level ascertained by golgin staining was also observed in other cell types. Specificity of the phenotype was indicated by the indistinguishable results observed, with siRNAs targeting regions corresponding to three distinct exons of golgin-160, exons 15, 19, and 23, and, as previously published (Rios *et al.*, 2004), two distinct regions of GMAP210. Interestingly, golgin-160 is alternatively spliced (Hicks and Machamer, 2005) and siRNAs targeting exon 5 fail to induce Golgi fragmentation (Hicks *et al.*, 2006; Williams *et al.*, 2006), suggesting that golgin-160 transcripts lacking exon 5,

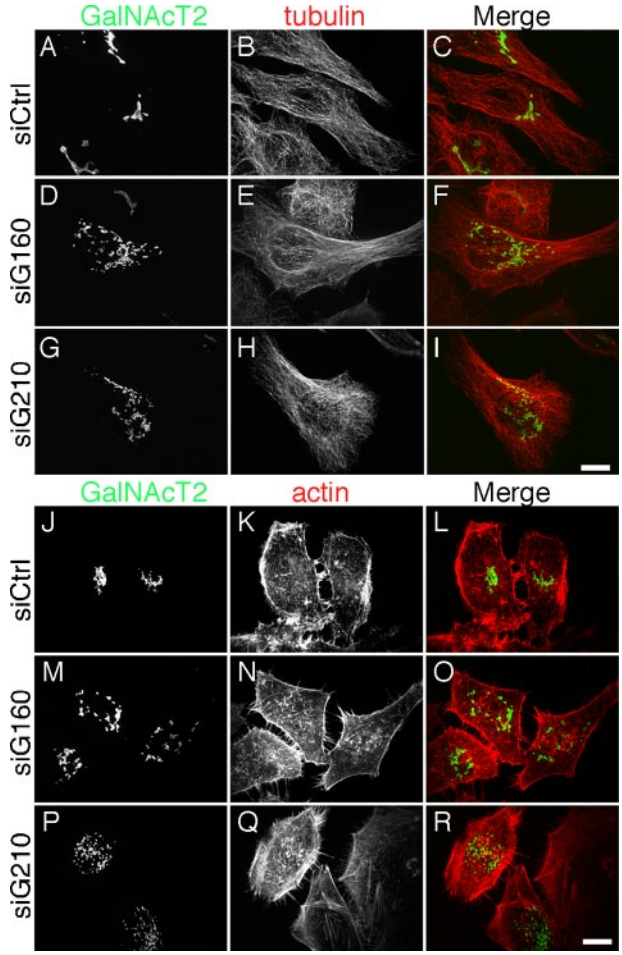

Figure 3. Integrity of the microtubule and actin cytoskeleton. (A–I) The microtubule cytoskeleton was examined in cells 72 h after treatment with control siRNA (A–C), golgin-160 siRNA (D–F), or GMAP210 siRNA (G–I) and then imaged to reveal the Golgi (GalNAcT2-GFP) and tubulin staining. Merged images are also shown. Bar, 10 μm. (J–R) The actin cytoskeleton was examined in cells treated as above (A–I) and imaged to reveal the Golgi (GalNAcT2-GFP) and phalloidin staining. Bar, 10 μm.

which have been detected (e.g., transcript 00000058369, http://www.ebi.ac.uk/), may partially support its function. In any case, the dispersed Golgi phenotype described here was a consequence of loss of golgin-160 function and was reversed by expression of a full-length golgin-160 replacement construct (Supplemental Figure S1). Knockdown as determined by immunoblot confirmed that control proteins were unaffected and that neither knockdown affected the level of the other golgin (Figure 1J). Compared with control cells, the average number of distinct fluorescent Golgi objects was increased by 10-fold in cells depleted of golgin-160 or GMAP210 (Figure 1K). Transmission electron microscopy analysis revealed that the dispersed Golgi membranes in golgin-160 and GMAP210 knockdown cells were dispersed ministacks similar to those present in nocodazole-treated cells (Figure 2, A–D). In the thin sections obtained, which typically encompassed only a fraction of the full ribbon in control cells and therefore underestimated its length, the observed ribbon length was decreased by 10-fold to ~0.2 μm. The presence of ministacks suggests maintenance of compartmentalization, and this was consistent with a fluorescence analysis showing that marker segregation was maintained in the Golgi membranes of the knockdown cells (Figure 2, E–Q). Thus, Golgi organization with respect to fragmentation, stacking and separation of markers argues that depletion of golgin-160 or GMAP210 yields a phenotype in which the Golgi ribbon is fragmented into distributed ministacks.

Having identified two knockdown conditions that block Golgi positioning at the MTOC, we next needed to confirm that the microtubule and actin cytoskeleton remained assembled. Golgi and tubulin costaining indicated that despite the dispersed Golgi, the knockdown cells contained intact microtubule arrays indistinguishable from controls (Figure 3, A–I). A microtubule reassembly assay was also used in these cells to assess microtubule growth from the MTOC and, again, no difference was observed between control and golgin-160 or GMAP210 knockdown cells. With similar time courses, single prominent microtubule asters were formed emanating from juxtanuclear positions (not shown). Further, actin stress fibers and filopodial actin assemblies were present and apparently unaltered in cells after knockdown of either golgin (Figure 3, J–R). Thus, loss of Golgi positioning in the knockdown cells could not be attributed to defects in cytoskeletal organization arguing that golgin-160 and GMAP210 more directly participate in Golgi positioning. Next, live imaging was used to assay centripetal movement

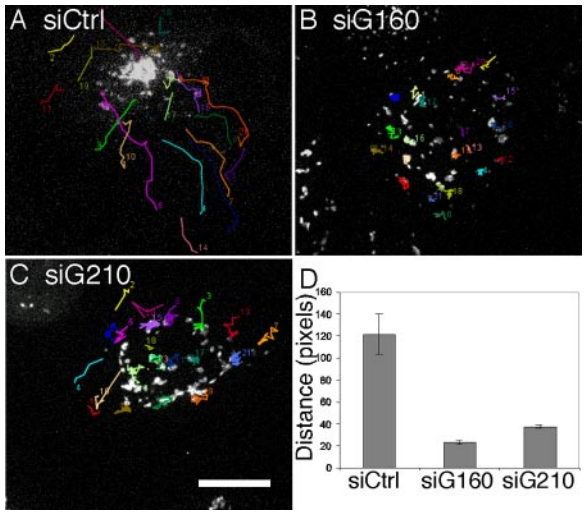

Figure 4. Golgin-160 and GMAP210 are required for Golgi membrane motility. (A–D) GalNAcT2-expressing cells were treated with control siRNA (A), golgin-160 siRNA (B), or GMAP210 siRNA (C), and then live imaging was carried after nocodazole washout. Nocodazole treatment was at 0.5 μg/ml for 3 h and washout was initiated by perfusion with fresh growth medium. Excerpted frames show final time points overlaid by tracks indicating frame-by-frame movement of Golgi objects during the entire imaging period. Bar, 10 μm. See Supplemental Material for the original movies. Golgi object movement was quantified for each condition by determining the net displacement of each object from the first to last frame (D). Average values are plotted (±SEM, n = 3).

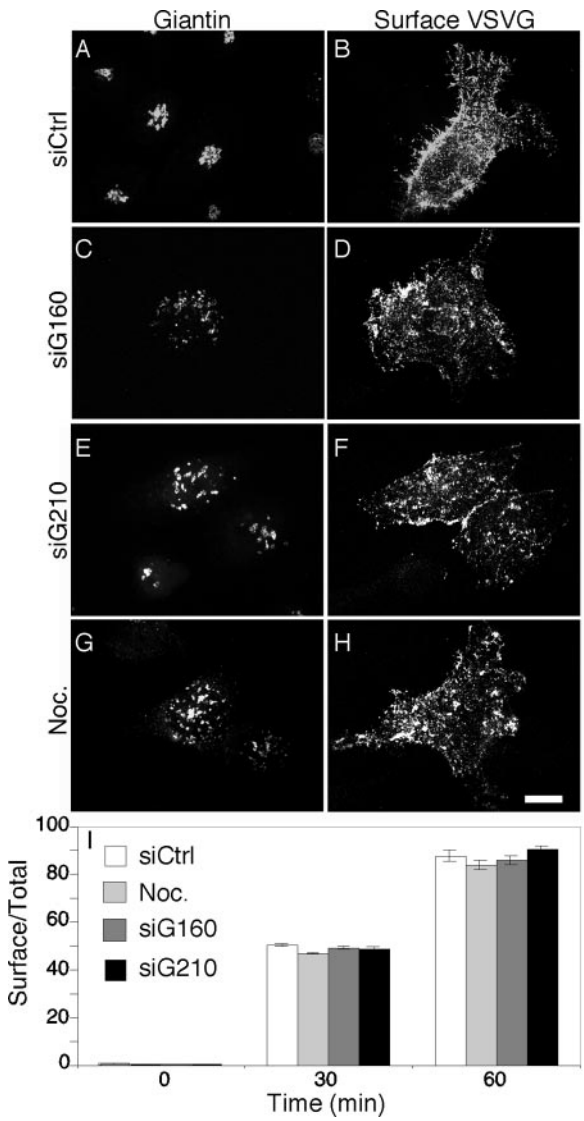

Figure 5. ER to surface trafficking of VSVG-GFP. (A–I) Control siRNA- (A and B), golgin-160 siRNA- (C and D), GMAP210 siRNA- (E and F), and nocodazole- (G and H) treated HeLa cells stably expressing ts045 VSVG-GFP were shifted to the permissive temperature for VSVG trafficking for 60 min before staining surface-exposed VSVG. After fixation the cells were stained using anti-giantin antibodies to reveal the Golgi structure. The plot shows the ratio of surface to total VSVG-GFP fluorescence for the indicated time points (I).

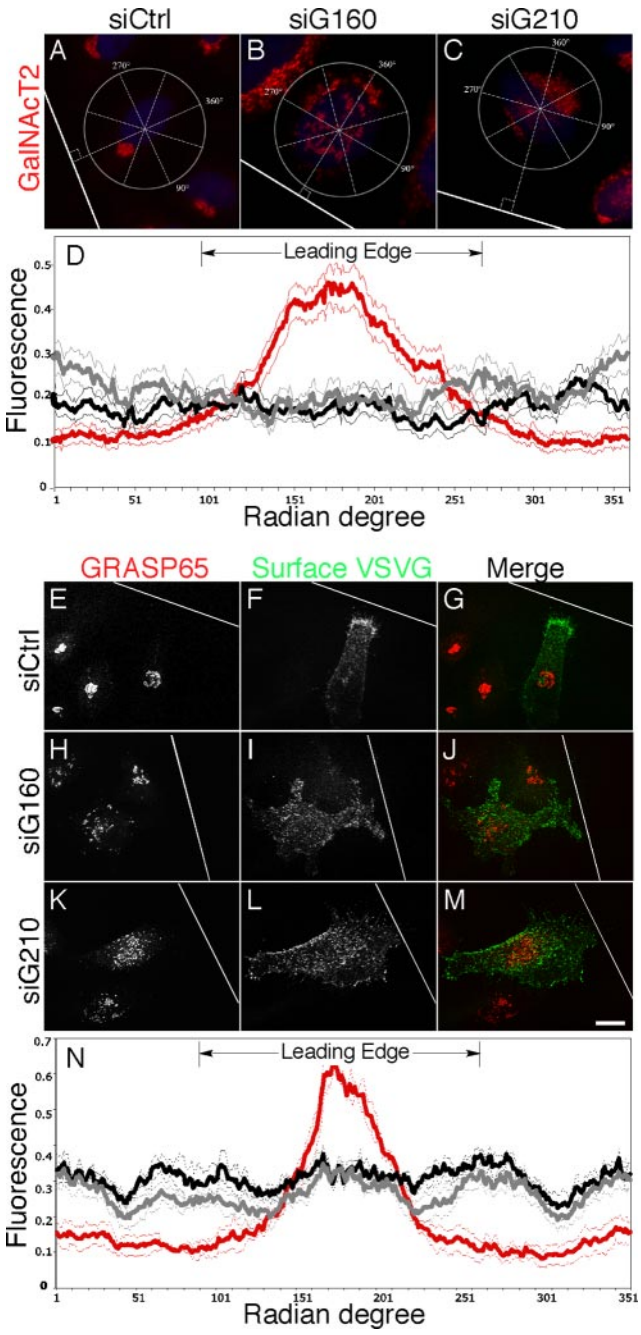

Figure 6. Golgi dispersal associates with impaired polarized secretion. (A–C) HeLa cells expressing GalNAcT2-GFP and transfected with control siRNA (A), golgin-160 siRNA (B), or GMAP210 siRNA (C) were wounded and, after 6 h the Golgi (GalNAcT2-GFP in red) and the nuclei (Hoechst staining in blue) were imaged. White line indicates wound edge. Examples of best-fit circles and quadrants with the 180° radian perpendicular to the wound edge are shown. Bar, 10 μm. (D) Golgi position polarity was quantified by plotting the normalized intensity of GalNAcT2-GFP fluorescence for each degree radian of the best-fitting circle. The hemicycle facing the leading edge is indicated. Values are averages (±SEM, n = 3) with control, golgin-160, and GMAP210 siRNA treatments plotted in red, black, and gray, respectively. (E–M) HeLa cells were transfected with control siRNA (E–G), golgin-160 siRNA (H–J), or GMAP210 siRNA (K–M), and then, after 52 h the cells were induced at 40°C with doxycycline to accumulate VSVG-GFP in the ER for 20 h. Then the cells were wounded (white line indicates wound edge), and after 6 h the cells were incubated at the permissive temperature for 30 min and processed to reveal surface VSVG staining and localization of the Golgi marker GRASP65. Bar, 10 μm. (N) Secretion polarity was quantified by plotting the normalized intensity of VSVG-GFP surface staining for each degree radian of the best-fitting circle encompassing the cell. Radian degrees corresponding to the leading edge are indicated. Values are averages (±SEM, n = 3) with control, golgin-160, and GMAP210 siRNA treatments plotted in red, black, and gray, respectively.

of Golgi membranes during microtubule reassembly. In contrast to control cells in which rapid and sustained inward movements of Golgi elements ultimately reestablished the juxtanuclear Golgi ribbon, such movements were rarely observed in cells treated with siRNA targeting either golgin (Figure 4, A–C, and Supplemental Material, Movies 1–3). In these cells, the Golgi membranes mostly retained their peripheral location as indicated by a determination of the net displacement of each Golgi object over the course of the imaging periods (Figure 4D).

Not only was the cytoskeleton intact in the golgin-depleted cells but secretion also appeared normal as measured using ER-to-surface transport of the temperature-sensitive mutant of the VSVG-GFP. VSVG-GFP was detected at the cell surface using an anti-ectodomain antibody within 20 min after shift to permissive temperature and, despite the presence of a dispersed Golgi apparatus, surface VSVG-GFP accumulated with kinetics indistinguishable from that of controls (Figure 5, A–I). As an alternative assay of membrane transport, Golgi reassembly was examined upon washout of brefeldin A (BFA), which inhibits Arf1 activation and causes collapse of the Golgi apparatus and redistribution of Golgi-localized proteins to the ER and to remnant structures (Donaldson *et al.*, 1992). Knockdown cells depleted of either golgin-160 or GMAP210 behaved in a manner similar to controls in that GalNAcT2-GFP redistributed to the ER upon BFA treatment and BFA washout was accompanied by the rapid emergence of GalNAcT2-GFP from the ER and its apparent concentration in post-ER membranes (Supplemental Figure S2). As expected, the reassembled membranes failed to move inward and form a Golgi ribbon, but the rates of ER export, estimated using image analysis, were similar to controls.

Although elucidation of the precise role of golgin-160 and GMAP210 in Golgi membrane motility is an important focus of future work, the above experiments indicate that cells depleted of either golgin lose peri-centrosomal Golgi positioning, whereas retaining normal secretion kinetics and cytoskeletal structure, thus establishing conditions to test the specific role of Golgi positioning on directed secretion and cell polarity. Toward this end, scratch wounding was carried out on control cells and cells depleted of either golgin. As expected (Kupfer *et al.*, 1982; Bergmann *et al.*, 1983), control cells oriented the juxtanuclear Golgi ribbon toward the wound edge, but Golgi orientation was not evident in cells depleted of golgin-160 or GMAP210 (Figure 6, A–C). By assaying the normalized fluorescence at each degree radian for a best-fit circle of each cell, it was observed that Golgi fluorescence peaked in the leading edge hemicycle of controls, whereas no enrichment was evident in the knockdown cells (Figure 6D). Significantly, after a 30-min release from the restrictive temperature, newly inserted surface VSVG-GFP was strongly enriched at the cell leading edge (Figure 6, E–G). In striking contrast, newly inserted surface VSVG-GFP was not enriched at the leading edge in the golgin-depleted cells and instead was uniform (Figure 6, H–M). Assaying the normalized fluorescence at each degree

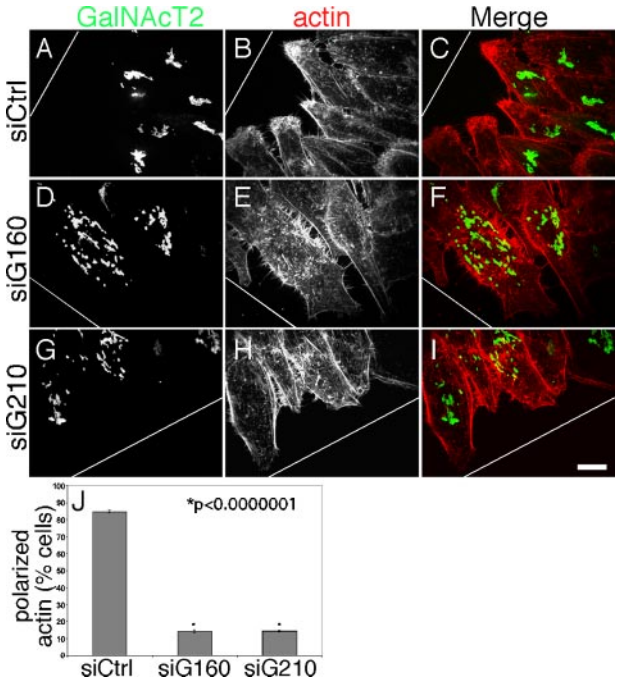

Figure 7. Actin loses its asymmetric localization in the absence of Golgi pericentrosomal positioning. (A–I) HeLa cells expressing GalNAcT2-GFP and transfected with control siRNA (A–C), golgin-160 siRNA (D–F), or GMAP210 siRNA (G–I) were wounded and, after 6 h, were stained with phalloidin to visualize the polymerized actin network. White line indicates wound edge. Bar, 10 μm. (J) The percentage of cells at the wound edge with a polarized distribution of actin facing the leading edge is plotted. Values are averages (±SEM, n = 3).

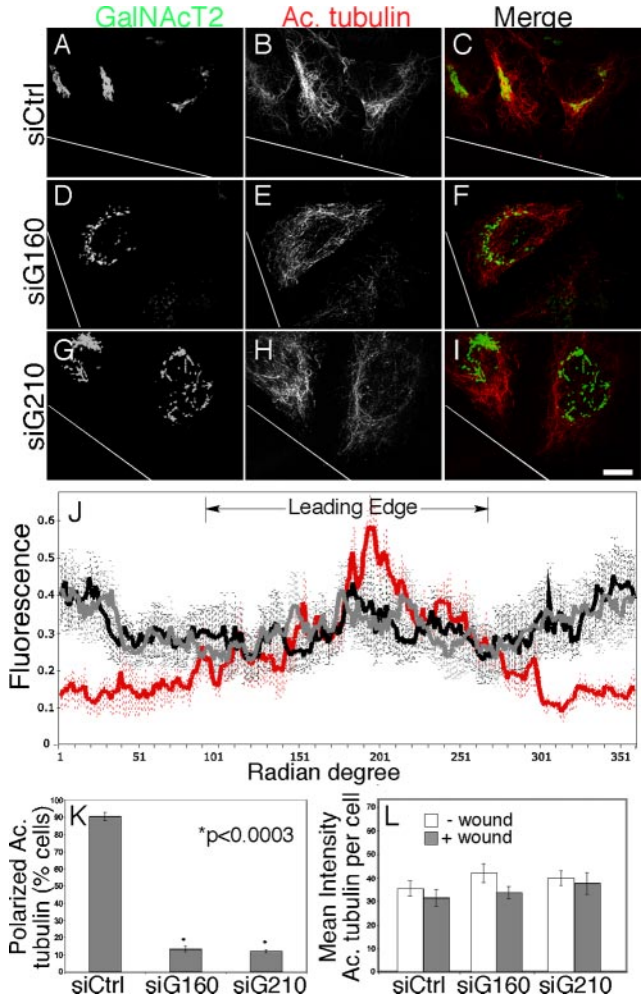

Figure 8. Randomized orientation of acetylated microtubules upon golgin knockdown. (A–I) HeLa cells expressing GalNAcT2-GFP were stained with an anti-acetylated tubulin antibody 72 h after transfection with control (A–C), golgin-160 (D–F), or GMAP210 (G–I) siRNA and 6 h after wounding. Bar, 10 μm. (J–L) Acetylated tubulin polarity was quantified by plotting the normalized intensity of staining for each degree radian of the best-fitting circle encompassing the cell (J). Radian degrees corresponding to the leading edge are indicated. Values are averages (±SEM, n = 3) with control, golgin-160, and GMAP210 siRNA treatments plotted in red, black, and gray, respectively. The percentage of cells with a wound edge oriented acetylated microtubule population is also plotted (K). Values are averages (±SEM, n = 3). The mean intensity of acetylated tubulin staining per cell in the absence of wounding and at the wound edge was also determined for each knockdown treatment (L). Golgin knockdown caused a randomization in orientation but not a loss of stable microtubules.

radian for each cell, it was determined that 70% of surface VSVG-GFP was present at the leading edge of controls, whereas no enrichment was evident in the knockdown cells (Figure 6N). Thus, polarized secretion in cells at the wound edge depends not only on an intact microtubule cytoskeleton but also on microtubule minus-end–directed motility of Golgi membranes positioning the Golgi apparatus at the MTOC.

Along with reorientation of the Golgi apparatus, hallmarks of cell polarization in response to a scratch-wound include accumulation of filamentous actin at the leading edge, centrosome reorientation, and accumulation of oriented, posttranslationally modified microtubules. As expected, each of these features was apparent after wounding cells treated with control siRNA. The Golgi apparatus faced the wound edge where there was a striking accumulation of actin (Figure 7, A–C), acetylated microtubules oriented toward the wound edge (Figure 8, A–C) and γ-tubulin staining marked centrosomal structures oriented to the wound (Supplemental Figure S3, A–C). In contrast, the cells at the wound edge depleted of golgin-160 or GMAP210 had distributed Golgi membranes and actin staining was much more uniformly distributed (Figure 7, D–J). Whereas ~85% of control cells exhibited polarized actin, this was reduced to ~15% in cells depleted of either golgin. Also, unlike in control cells where filopodial extensions were restricted to the leading edge upon wounding, filopodial extensions were seen all around the periphery of the knockdown cells.

Acetylated tubulin was also much more uniformly distributed in the golgin-depleted cells (Figure 8, D–I). Fluorescence analysis per degree radian over cells at the wound edge revealed that 68% of acetylated tubulin was oriented toward the wound in control cells, whereas no enrichment was evident in the knockdown cells (Figure 8J). Indeed, the fraction of cells exhibiting a polarized distribution of acetylated tubulin was reduced ninefold (Figure 8K). Quantification of the immunofluorescence images indicated that wounding did not increase the amount of acetylated microtubules per unit area across the entire cell nor did golgin knockdown cause a decrease (Figure 8L). Immunoblot analysis of nonwounded cells also confirmed that golgin knockdown did not block acetylated tubulin production (our unpublished results). Rather, in the knockdown cells the

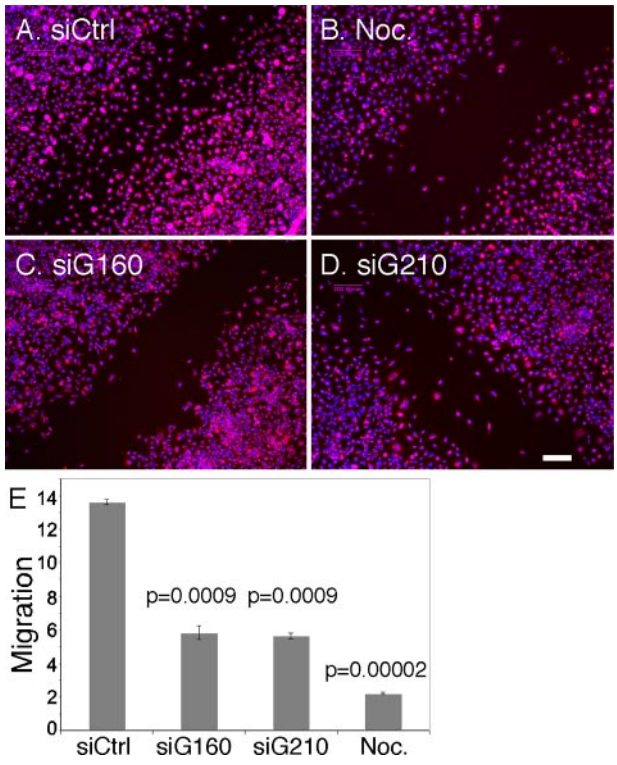

Figure 9. Wound healing is defective in cells with dispersed Golgi membranes. (A–D) HeLa cells treated with control siRNA (A), golgin-160 siRNA (C), or GMAP210 siRNA (D) were grown in a monolayer and wounded and, after 17 h, were fixed and processed to visualize the Golgi (Giantin) and nuclei (Hoechst shown in blue). The same experiment was also performed on nontransfected cells treated with 0.5 μg/ml nocodazole 3 h before wounding and during the wound healing incubation (B). Bar, 200 μm. (E) An estimate of migration speed (μm/h) for each condition is plotted. Values are averages ($\pm$SEM, n = 3).

acetylated microtubules were shorter and randomly oriented. The knockdown cells also had a randomized distribution of centrosomes relative to the wound (Supplemental Figure S3, D–I) such that reoriented centrosomes in response to wounding dropped from 90% in control cells to 23 and 24% in golgin-160 and GMAP210 knockdown cells, respectively (Supplemental Figure S3J).

The loss of cell polarity in terms of centrosome alignment, actin assembly, and stable microtubule distribution suggested that there would also be defects in cell migration during wound closure. Cells transfected with control siRNA moved into the wound area filling the gap created by the scratch within 16–18 h (Figure 9A). In contrast, cells treated with siRNA against golgin-160 (Figure 9C) or GMAP210 (Figure 9D) failed to close the gap in the same time period. As expected, nocodazole-treated cells, which were used as a positive control, exhibited negligible movement into the wound area (Figure 9B). The results were quantified by determining the rates of migration under each condition, and the analysis indicated a greater than 50% reduction in rate for the knockdown cells (Figure 9E). The impairment in wound healing was likely the consequence of a loss in directed migration rather than a loss of general cell motility because sparsely plated cells treated with the siRNAs remained motile. Thus, depletion of either golgin inhibited directed cell migration leading to a significant impairment in wound healing. These results show that directed secretion fails to occur when Golgi peri-centrosomal positioning is specifically blocked and that this inhibits cell polarization and cell migration.

DISCUSSION

Most mammalian cells position the Golgi apparatus near the centrosome-based MTOC. Nevertheless, in the absence of peri-centrosomal positioning, for example, in nonmammalian cells or after nocodazole treatment of mammalian cells, the Golgi is typically found organized into distributed ministacks, and these ministacks are fully functional in the core processing and sorting reactions carried out by the Golgi apparatus. What then is the functional significance of peri-centrosomal Golgi positioning? The present study identifies two conditions: inhibition of expression of golgin-160 or GMAP210, which alter Golgi positioning without disrupting secretion or the actin and microtubule networks. Significantly, the cells failed to polarize when stimulated by scratch wounding. Secretion was not focused toward the wound edge, actin failed to assemble at the wound edge, the centrosome and stable microtubules failed to orient toward the wound edge, and the cells failed to migrate in a directed manner into the wound area. Golgin-160 and GMAP210 did not colocalize within the Golgi (Figure 1), and they are not known to interact. The finding that establishment of polarity in response to wounding was blocked by inhibition of each of two proteins that appear to independently confer Golgi positioning argues strongly for a primary role of Golgi positioning in the wound response. Because previous tests failed to dissect the contributions of microtubule organization and Golgi positioning, these results provide the first direct demonstration that organization of the Golgi is critical in establishing directed secretion and the polarized state.

This work shows that both golgin-160 and GMAP210 are required for minus-end–directed motility of Golgi membranes. Based on the GMAP210 knockdown phenotype (Rios *et al.*, 2004), a role in motility had already been suggested (Linstedt, 2004), but the present work provides the first test of the hypothesis and also the first report of a similar role for golgin-160. GMAP210 has several significant but in some cases controversial activities that may participate in membrane motility. GMAP210 has been shown to bind Golgi membranes through its N-terminus, and its C-terminus binds γ-tubulin and localizes to centrosomes, leading to the hypothesis that it anchors Golgi membranes to centrosomes (Infante *et al.*, 1999; Rios *et al.*, 2004). However, others failed to observe Golgi localization of the N-terminus and have identified a "Grip-related Arf-binding domain" at the C-terminus that interacts with Golgi membranes and not centrosomes (Chen *et al.*, 1999; Gillingham *et al.*, 2004). Subsequently, a sequence motif termed "amphipathic lipid-packing sensor" was identified at the N-terminus that binds highly curved membranes and a construct comprised of the GMAP210 termini was shown to link vesicle-sized liposomes to larger liposomes in the presence of Arf1 and two Arf1 regulators, suggesting that GMAP210 tethers vesicles to Golgi membranes (Drin *et al.*, 2007, 2008). In the case of golgin-160, the N-terminus mediates Golgi localization (Hicks and Machamer, 2002) and golgin-160 interacts with the β1-adrenergic receptor, which depends on golgin-160 for efficient trafficking out of the Golgi (Hicks *et al.*, 2006). Golgin-160 also promotes surface expression of a subset of potassium channels and the targeting of a glucose transporter (Bundis *et al.*, 2006; Williams *et al.*, 2006). An important future direction is using gene replacement of mutated forms of the golgins after siRNA-mediated knockdown (Pu-

thenveedu and Linstedt, 2004) to determine which of the known activities are functionally required for Golgi membrane motility in living cells.

Although an aligned Golgi position shortens the distance between sites of vesicle budding at the TGN and sites of vesicle fusion at the leading edge, it is unlikely that proximity is the mechanism of directed secretion. Even though it is randomly oriented in the absence of wounding, or in cells behind the wound edge, the Golgi is still asymmetrically localized in these cells because of its peri-centrosomal location. Nevertheless, the plasma membrane domain faced by the Golgi did not accumulate VSVG-GFP (not shown) and, under these conditions, secretory vesicles have been shown to fuse at plasma membrane positions distributed across the entire cell (Schmoranzer *et al.*, 2000). Thus, directed secretion triggered by polarity cues depends on additional factors such as stabilized microtubules and localized vesicle targeting factors.

Stabilization of oriented microtubules increases the probability of directed delivery, and the probability may be further enhanced by a preference of the kinesin motor for stabilized microtubules (Reed *et al.*, 2006). Interestingly, the Golgi apparatus, itself, may nucleate stabilized microtubules oriented toward the leading edge through association with γ-tubulin and/or the microtubule-binding protein CLASP, and CLASP-deficient fibroblasts exhibit impaired directionally persistent migration (Akhmanova *et al.*, 2001; Chabin-Brion *et al.*, 2001; Drabek *et al.*, 2006; Efimov *et al.*, 2007). Thus, polarity cues that trigger Golgi reorientation would do so to build a network of stabilized microtubules focused on the leading edge. Reorientation of the Golgi was recently shown to depend on phosphorylation of the Golgi protein GRASP65, which likely fragments the Golgi to allow its movement (Bisel *et al.*, 2008). The results herein argue that Golgi fragmentation triggered by GRASP65 phosphorylation must be transient and minimal, probably a brief unlinking of the Golgi ribbon (Puthenveedu *et al.*, 2006; Feinstein and Linstedt, 2008), so that the reoriented Golgi membranes can reassemble a peri-centrosomal ribbon competent to establish polarized secretion.

The finding that cell polarity in response to a scratch wound requires positioning of the Golgi apparatus implies that after initiation by a polarity cue there is subsequent dependence on directed secretion to maintain the polarized state. Initiation and maintenance phases are present in other models of cell polarity (Drubin and Nelson, 1996). During wound healing, after upstream steps initiate localization of Cdc42-GTP, which is the central signaling molecule defining the wound edge, the polarized secretory apparatus may replenish factors involved in localized activation of Cdc42 or it may even deliver Cdc42 itself, as Cdc42-GTP is partially localized to Golgi membranes and its association with Golgi derived vesicles is up-regulated upon wounding (Etienne-Manneville, 2004). In sum, Golgi reorientation is part of a feedback loop that sustains the polarized state, and the cell polarity response can now be included among the growing list of signaling pathways that depend on structure, function, and localization of the Golgi apparatus.

ACKNOWLEDGMENTS

We thank Tim Feinstein for help initiating the project; Manojkumar Puthenveedu, Tina Lee, and Collin Bachert for critically reading the manuscript; Elmer Ker for cell migration assay assistance; Joe Suhan for the electron microscopy; and members of the Linstedt lab for thoughtful suggestions. We are indebted to C. Machamer (Johns Hopkins Medical School) for the golgin-160 plasmid and the anti-golgin-160 antibody. Funding was provided by National Institutes of Health Grant GM-56779 to A.D.L.

REFERENCES

Akhmanova, A. *et al.* (2001). Clasps are CLIP-115 and -170 associating proteins involved in the regional regulation of microtubule dynamics in motile fibroblasts. Cell *104*, 923–935.

Barr, F. A., and Short, B. (2003). Golgins in the structure and dynamics of the Golgi apparatus. Curr. Opin. Cell Biol. *15*, 405–413.

Bergmann, J. E., Kupfer, A., and Singer, S. J. (1983). Membrane insertion at the leading edge of motile fibroblasts. Proc. Natl. Acad Sci. USA *80*, 1367–1371.

Bershadsky, A. D., and Futerman, A. H. (1994). Disruption of the Golgi apparatus by brefeldin A blocks cell polarization and inhibits directed cell migration. Proc. Natl. Acad Sci. USA *91*, 5686–5689.

Bisel, B., Wang, Y., Wei, J. H., Xiang, Y., Tang, D., Miron-Mendoza, M., Yoshimura, S., Nakamura, N., and Seemann, J. (2008). ERK regulates Golgi and centrosome orientation towards the leading edge through GRASP65. J. Cell Biol. *182*, 837–843.

Bundis, F., Neagoe, I., Schwappach, B., and Steinmeyer, K. (2006). Involvement of Golgin-160 in cell surface transport of renal ROMK channel: co-expression of Golgin-160 increases ROMK currents. Cell Physiol. Biochem. *17*, 1–12.

Burkhardt, J. K., Echeverri, C. J., Nilsson, T., and Vallee, R. B. (1997). Overexpression of the dynamitin (p50) subunit of the dynactin complex disrupts dynein-dependent maintenance of membrane organelle distribution. J. Cell Biol. *139*, 469–484.

Chabin-Brion, K., Marceiller, J., Perez, F., Settegrana, C., Drechou, A., Durand, G., and Pous, C. (2001). The Golgi complex is a microtubule-organizing organelle. Mol. Biol. Cell *12*, 2047–2060.

Chen, Y., Chen, P. L., Chen, C. F., Sharp, Z. D., and Lee, W. H. (1999). Thyroid hormone, T3-dependent phosphorylation and translocation of Trip230 from the Golgi complex to the nucleus. Proc. Natl. Acad Sci. USA *96*, 4443–4448.

de Anda, F. C., Pollarolo, G., Da Silva, J. S., Camoletto, P. G., Feiguin, F., and Dotti, C. G. (2005). Centrosome localization determines neuronal polarity. Nature *436*, 704–708.

Donaldson, J. G., Finazzi, D., and Klausner, R. D. (1992). Brefeldin A inhibits Golgi membrane-catalysed exchange of guanine nucleotide onto ARF protein. Nature *360*, 350–352.

Drabek, K. *et al.* (2006). Role of CLASP2 in microtubule stabilization and the regulation of persistent motility. Curr. Biol. *16*, 2259–2264.

Drin, G., Casella, J. F., Gautier, R., Boehmer, T., Schwartz, T. U., and Antonny, B. (2007). A general amphipathic alpha-helical motif for sensing membrane curvature. Nat. Struct. Mol. Biol. *14*, 138–146.

Drin, G., Morello, V., Casella, J. F., Gounon, P., and Antonny, B. (2008). Asymmetric tethering of flat and curved lipid membranes by a golgin. Science *320*, 670–673.

Drubin, D. G., and Nelson, W. J. (1996). Origins of cell polarity. Cell *84*, 335–344.

Efimov, A. *et al.* (2007). Asymmetric CLASP-dependent nucleation of noncentrosomal microtubules at the trans-Golgi network. Dev. Cell *12*, 917–930.

Etienne-Manneville, S. (2004). Cdc42—the centre of polarity. J. Cell Sci. *117*, 1291–1300.

Feinstein, T. N., and Linstedt, A. D. (2008). GRASP55 regulates Golgi ribbon formation. Mol. Biol. Cell *19*, 2696–2707.

Gillingham, A. K., Tong, A. H., Boone, C., and Munro, S. (2004). The GTPase Arf1p and the ER to Golgi cargo receptor Erv14p cooperate to recruit the golgin Rud3p to the cis-Golgi. J. Cell Biol. *167*, 281–292.

Goldman, R. D. (1971). The role of three cytoplasmic fibers in BHK-21 cell motility. I. Microtubules and the effects of colchicine. J. Cell Biol. *51*, 752–762.

Hicks, S. W., Horn, T. A., McCaffery, J. M., Zuckerman, D. M., and Machamer, C. E. (2006). Golgin-160 promotes cell surface expression of the beta-1 adrenergic receptor. Traffic *7*, 1666–1677.

Hicks, S. W., and Machamer, C. E. (2002). The NH2-terminal domain of Golgin-160 contains both Golgi and nuclear targeting information. J. Biol. Chem. *277*, 35833–35839.

Hicks, S. W., and Machamer, C. E. (2005). Isoform-specific interaction of golgin-160 with the Golgi-associated protein PIST. J. Biol. Chem. *280*, 28944–28951.

Infante, C., Ramos-Morales, F., Fedriani, C., Bornens, M., and Rios, R. M. (1999). GMAP-210, A cis-Golgi network-associated protein, is a minus end microtubule-binding protein. J. Cell Biol. *145*, 83–98.

King, S. J., and Schroer, T. A. (2000). Dynactin increases the processivity of the cytoplasmic dynein motor. Nat. Cell Biol. *2*, 20–24.

Kupfer, A., Dennert, G., and Singer, S. J. (1983). Polarization of the Golgi apparatus and the microtubule-organizing center within cloned natural killer cells bound to their targets. Proc. Natl. Acad Sci. USA *80*, 7224–7228.

Kupfer, A., Louvard, D., and Singer, S. J. (1982). Polarization of the Golgi apparatus and the microtubule-organizing center in cultured fibroblasts at the edge of an experimental wound. Proc. Natl. Acad Sci. USA *79*, 2603–2607.

Linstedt, A. D. (2004). Positioning the Golgi apparatus. Cell *118*, 271–272.

Linstedt, A. D., Mehta, A., Suhan, J., Reggio, H., and Hauri, H. P. (1997). Sequence and overexpression of GPP130/GIMPc: evidence for saturable pH-sensitive targeting of a type II early Golgi membrane protein. Mol. Biol. Cell *8*, 1073–1087.

Preisinger, C., Short, B., De Corte, V., Bruyneel, E., Haas, A., Kopajtich, R., Gettemans, J., and Barr, F. A. (2004). YSK1 is activated by the Golgi matrix protein GM130 and plays a role in cell migration through its substrate 14-3-3zeta. J. Cell Biol. *164*, 1009–1020.

Prigozhina, N. L., and Waterman-Storer, C. M. (2004). Protein kinase D-mediated anterograde membrane trafficking is required for fibroblast motility. Curr. Biol. *14*, 88–98.

Pu, J., and Zhao, M. (2005). Golgi polarization in a strong electric field. J. Cell Sci. *118*, 1117–1128.

Puthenveedu, M.A., Bachert, C., Puri, S., Lanni, F., and Linstedt, A.D. (2006). GM130 and GRASP65-dependent lateral cisternal fusion allows uniform Golgi-enzyme distribution. Nat. Cell Biol. *8*, 238–248.

Puthenveedu, M. A., and Linstedt, A. D. (2004). Gene replacement reveals that p115/SNARE interactions are essential for Golgi biogenesis. Proc. Natl. Acad Sci. USA *101*, 1253–1256.

Reed, N. A., Cai, D., Blasius, T. L., Jih, G. T., Meyhofer, E., Gaertig, J., and Verhey, K. J. (2006). Microtubule acetylation promotes kinesin-1 binding and transport. Curr. Biol. *16*, 2166–2172.

Rios, R. M., Sanchis, A., Tassin, A. M., Fedriani, C., and Bornens, M. (2004). GMAP-210 recruits gamma-tubulin complexes to cis-Golgi membranes and is required for Golgi ribbon formation. Cell *118*, 323–335.

Rodionov, V. I., Gyoeva, F. K., Tanaka, E., Bershadsky, A. D., Vasiliev, J. M., and Gelfand, V. I. (1993). Microtubule-dependent control of cell shape and pseudopodial activity is inhibited by the antibody to kinesin motor domain. J. Cell Biol. *123*, 1811–1820.

Roghi, C., and Allan, V.J. (1999). Dynamic association of cytoplasmic dynein heavy chain 1a with the Golgi apparatus and intermediate compartment. J. Cell Sci. *112*(Pt 24), 4673–4685.

Schmoranzer, J., Goulian, M., Axelrod, D., and Simon, S. M. (2000). Imaging constitutive exocytosis with total internal reflection fluorescence microscopy. J. Cell Biol. *149*, 23–32.

Schmoranzer, J., Kreitzer, G., and Simon, S. M. (2003). Migrating fibroblasts perform polarized, microtubule-dependent exocytosis towards the leading edge. J. Cell Sci. *116*, 4513–4519.

Takahashi, M., Shibata, H., Shimakawa, M., Miyamoto, M., Mukai, H., and Ono, Y. (1999). Characterization of a novel giant scaffolding protein, CG-NAP, that anchors multiple signaling enzymes to centrosome and the golgi apparatus. J. Biol. Chem. *274*, 17267–17274.

Thyberg, J., and Moskalewski, S. (1999). Role of microtubules in the organization of the Golgi complex. Exp. Cell Res. *246*, 263–279.

Vasiliev, J. M., Gelfand, I. M., Domnina, L. V., Ivanova, O. Y., Komm, S. G., and Olshevskaja, L. V. (1970). Effect of colcemid on the locomotory behaviour of fibroblasts. J. Embryol. Exp. Morphol. *24*, 625–640.

Vaughan, P. S., Miura, P., Henderson, M., Byrne, B., and Vaughan, K. T. (2002). A role for regulated binding of p150(Glued) to microtubule plus ends in organelle transport. J. Cell Biol. *158*, 305–319.

Williams, D., Hicks, S. W., Machamer, C. E., and Pessin, J. E. (2006). Golgin-160 is required for the Golgi membrane sorting of the insulin-responsive glucose transporter GLUT4 in adipocytes. Mol. Biol. Cell *17*, 5346–5355.